The Effects of Scattering Angle and Cumulus Cloud Geometry on Satellite Retrievals of Cloud Droplet Effective Radius

Brian Vant-Hull, Alexander Marshak, Lorraine A. Remer, and Zhanqing Li

***Abstract*—The effect of scattering angle on Moderate Resolution Imaging Spectroradiometer (MODIS) retrievals of cloud drop effective radius is studied using ensembles of cumulus clouds with varying sun–satellite scattering geometries. The results are interpreted as shadowing and illumination effects. When 3-D clouds are viewed near the backscatter geometry, well-illuminated cloud surfaces are seen, and the retrievals based on plane-parallel geometry underestimate the effective radius. The reverse is true when the satellite is far from the backscatter position, and the shadowed portions of clouds are observed. The shadowing geometry produces a larger bias than the illuminated geometry. These differences between the shadowed and the illuminated ensembles decrease toward zero as the clouds become shallower. Removing the edge pixels based on 1-km-scale geometry partially reduces biases due to the 3-D effects and surface contamination. Recommendations are provided for reducing the 3-D cloud effects using current satellite retrieval algorithms.**

***Index Terms*—Clouds, remote sensing, terrestrial atmosphere.**

I. Introduction

SATELLITE studies of cloud microphysics are important for understanding precipitation processes [1] and for climatic studies involving radiation transfer [2]. Although satellites allow large-scale spatial studies with large data ensembles, they suffer from the limitations of viewing a 3-D system from a single-point perspective at pixel resolution. All remote sensing operational retrievals of cloud properties assume plane-parallel geometry with pixels that are radiatively independent of their neighbors (e.g., [3]). Here, we examine the application of the widely used algorithm of Nakajima and King [4] to cumulus clouds, allowing retrieval of cloud drop effective radius and optical thickness from the reflectance in the visible and near-infrared (NIR) spectral regions.

Manuscript received June 29, 2006; revised October 11, 2006. This work was supported in part by the NASA Goddard Graduate Student Research Program, in part by the Department of Energy under Grant DE-A105-90ER61069 as part of the Atmospheric Radiation Measurement program, in part by NASA's Radiation Program Office under Grants 631-30-86 and 622-42-57, and in part by the National Science Foundation under Grant ATM0425069.

B. Vant-Hull is with the Department of Atmospheric and Oceanic Sciences, University of Maryland, College Park, MD 20741 USA (e-mail: brianvh@atmos.umd.edu).

A. Marshak and L. A. Remer are with the NASA Goddard Climate and Radiation Branch, Greenbelt, MD 20771 USA (e-mail: marshak@climate.gsfc.nasa.gov; lorraine.a.remer@nasa.gov).

Z. Li is with the Department of Atmospheric and Oceanic Science and the Earth System Science Interdisciplinary Center, University of Maryland, College Park, MD 20741 USA (e-mail: zli@atmos.umd.edu).

Color versions of one or more of the figures in this paper are available online at http://ieeexplore.ieee.org.

Digital Object Identifier 10.1109/TGRS.2006.890416

The above technique is best applied to stratus or stratocumulus clouds that are well approximated by plane-parallel geometry. Most cumulus clouds cannot be described as plane parallel at the 1-km resolution, which is typical of many satellite studies. A number of studies have addressed the effect of inaccurate assumptions about cloud geometry on the operational retrievals of cloud properties [5]–[10], and others have attempted to create retrievals that are fully 3-D [11], [12]. However, these techniques are not yet developed for use in operational retrievals.

Despite the possible inaccuracies, the plane-parallel approximations are still applied to cumulus clouds. A simple way to reduce the 3-D biases is to remove the cloud edge pixels [22] and maintain a view angle near nadir. Kaufman and Fraser [13] applied this technique with the Nakajima–King algorithm to calculate the aerosol indirect effect of smoke on the cloud effective radius in Brazil. In the same region, Feingold *et al.* [14] used a similar retrieval with a data analysis based on fractional rather than absolute changes in cloud and aerosol properties in order to cancel out the systematic retrieval biases. Both studies employed a large data set to suppress the random retrieval errors. Yet, even if the reflectance variations due to the cloud geometry are randomly distributed, the retrieval algorithms are nonlinear and tend to skew any original symmetry in the data set [9]. To further improve the accuracy of the preceding studies, it is necessary to explore the nature of 3-D biases once the retrieval algorithms have been applied. Using a data set similar to those above, this paper investigates the effects that cloud geometry and relative orientations of sun and satellite have on the standard plane-parallel retrievals of cloud drop effective radius, shedding light on the size and trend of these biases.

Although cloud optical thickness is retrieved simultaneously with the effective radius, its relationship with the variable illumination of 3-D clouds (brighter pixels mimic higher optical thickness) has been the topic of several past studies [5], [7], [8]. Here, we focus exclusively on the retrievals of effective radius.

II. Theory: Shadowing, Illumination, and Scattering Angle

In a plane-parallel approximation, it is assumed that the solar radiation uniformly illuminates the tops of the clouds, and that satellites only view this top-reflected radiation. In addition, it is assumed that the radiation emanating from one pixel is independent of its neighbors. As a result, shadowing and illumination

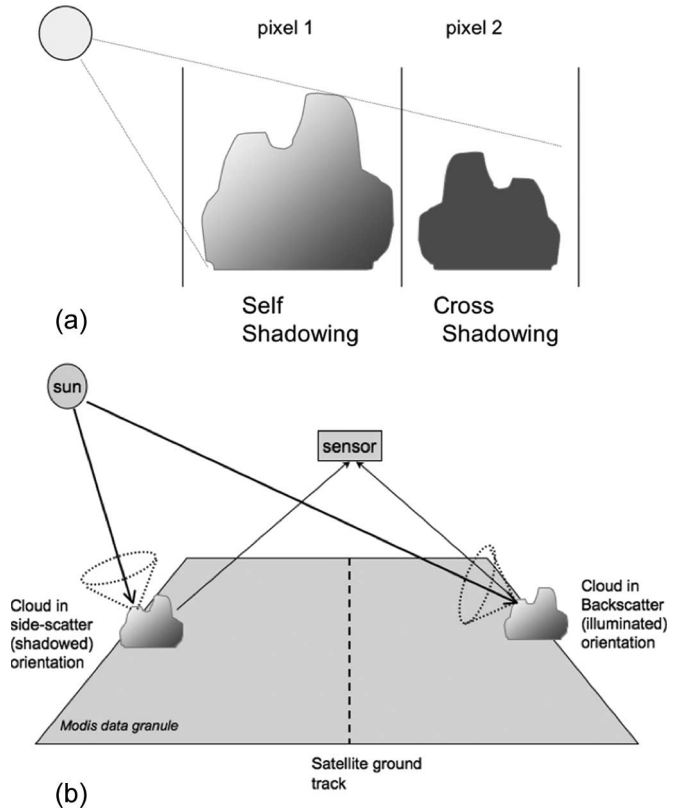

Fig. 1. Cloud shadowing. (a) Cartoon demonstrating the difference between self-shadowing and cross shadowing for cumulus clouds. (b) Relationship between the sun and sensor locations and the division of data into backscatter and sidescatter geometries. The cones drawn in dotted lines indicate the range of angles within which the sun and satellite are considered to be in the backscatter geometry. If both vectors are not within the cone, the cloud is classified as being in the sidescatter geometry.

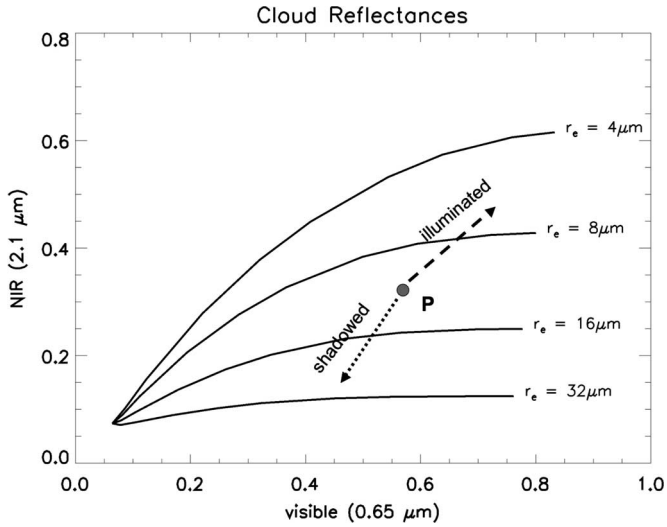

Fig. 2. Visible (0.65 μm) and NIR (2.1 μm) reflectance from the plane-parallel clouds for various values of effective radius. The satellite is at nadir; the sun is at a zenith of 25°. The surface reflectance due to vegetation is assumed to be 0.05 in the visible and 0.08 in the NIR (adapted from Varnai and Marshak [8]).

are not accounted for. For a nonplane-parallel cloud, the surface will experience varying amounts of shadow and illumination due to local orientation to the sun and/or obstruction by other parts of the cloud. Fig. 1(a) shows two neighboring cloud-filled pixels illuminated from the left. For the left cloud, the side facing away from the sun is in shadow; this will be referred to as "self-shadowing." The amount of shadow viewed will depend on the location of the sensor relative to the sun. Note that this is a subpixel phenomenon stemming from geometrical features not resolved by satellite. A different type of shadowing is illustrated by the pixel on the right that is blocked from illumination by the pixel with higher cloud tops on the left; this will be referred to as "cross shadowing." Therefore, as long as it is not blocked from view, cross shadowing of an individual pixel is independent of the sensor location. The amount of cross shadowing can be predicted from the resolved (pixel resolution) geometry of the clouds [8], [9]. In practical terms, the difference between the unresolved and resolved variability means that the amount of self-(cross) shadowing viewed by the satellite depends strongly(weakly) on the sensor location relative to the sun.

This paper is concerned primarily with self-shadowing. The distinction can be important: the only other observational studies, we are aware of, that investigated the effects of shadowing on cloud drop effective radius retrievals discussed cross shadowing only and ignored the sensor location [8], [9]. Yet, all pixels containing 3-D clouds are subject to self-shadowing, while cross shadowing only occurs if the neighboring pixels on the sunward side have higher cloud tops. The effects of self-shadowing may be controlled by the scattering angle: if the sensor is in the direct backscatter location, it will view only the illuminated portions of the clouds; away from the backscatter position, it will view increasingly the shadowed portions. This is shown in Fig. 1(b) in which the sensor will view the shadowed or illuminated portions of the clouds depending on the location of the sun and satellite relative to the pixel. For an ensemble of similar clouds, the resulting 3-D effects will vary smoothly between these positions.

The effects of shadowing and illumination on the effective radius (r_{e}) retrieval may be understood by referring to Fig. 2, which shows the Nakajima–King [4] lookup table for visible (0.67 μm) and NIR (2.1 μm) reflectance from plane-parallel clouds. To create each contour, radiative transfer calculations were performed for clouds with the labeled values of effective radius over a vegetated surface, and the optical thickness varied from 1 to 64 to produce the range of reflectances shown. Point P represents the reflectances expected for a plane-parallel cloud of a given optical depth and effective radius. If the local surface is tilted toward the sun, both reflectances will increase, as shown by the dashed line (illumination), and the retrieved value of r_{e} decreases [8]. If the local surface is tilted away from the sun, the reflectances will decrease (shadowing), and the NIR will decrease more than the visible due to absorption, as shown by the dotted line. This results in an increase of the retrieved value of r_{e}. Shadowing (illumination) thus causes overestimation (underestimation) of the retrieved effective radius relative to the physically correct value.

The retrieval of r_{e} is nonlinear, and for a random distribution of illumination and shadowing, there is no reason to expect the errors to cancel out. For the optically thick clouds (right side of Fig. 2), the values of r_{e} are nearly independent of the visible

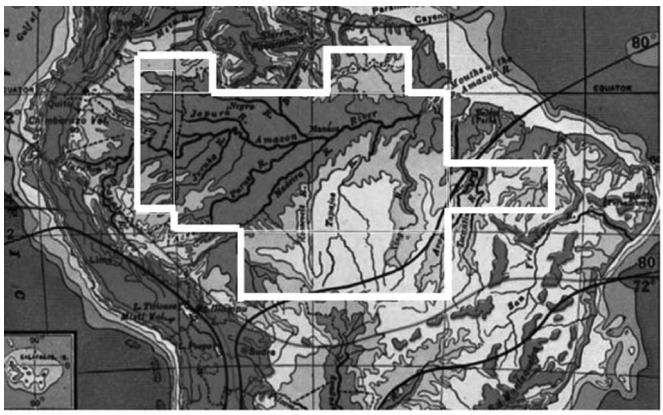

Fig. 3. Region used in this paper.

reflectance. For the nearly and equally spaced values of NIR reflectance shown, the values of r_e form a geometrical sequence, and the average value of r_e across a random set of observations would likely be biased higher than that of the plane-parallel case [9]. Satellite viewing geometry is rarely random, so the distribution of scattering angles must be investigated for each ensemble separately.

Three-dimensional clouds often do not uniformly fill a pixel. Because the vegetated surface is darker at 2.1 μm than a cloud, allowing partial filling of the "cloud pixel" with surface reflectance will increase the retrieved value of r_e [15]. A recent modeling study indicates that for small clouds, contamination from a dark surface can dominate scattering angle effects, so that r_e is always overestimated [10]. The ensemble average geometry of shadowed and illuminated sets of clouds should be equivalent, so we assume that surface contamination introduces a constant positive bias to all data set averages with the same environmental parameters.

III. Data and Method

An ideal demonstration of the effect of scattering angle on cloud effective radius retrievals would employ a multitude of sensors placed at different scattering angles looking at the same set of clouds. A more feasible alternative is a single sensor making an ensemble of observations of clouds in similar environmental conditions but with different scattering angles. Cloud variability produces noise in the observed data, but large ensembles reduce the signal-to-noise ratio if the environment is suitably constrained.

The Moderate Resolution Imaging Spectrometer (MODIS) Aqua satellite was used to observe clouds over the Amazon basin in August through October of 2002, which is an area of approximately 3 million km^2. Regions that border the coast or that correspond to topographical elevations above 500 m were avoided, as shown in Fig. 3. The MODIS level 2 collection 4 operational products were used to retrieve all the data used in this paper [16]–[18]. The 1-km cloud mask at the highest confidence level was employed to define the horizontal geometry of the cloud fields (average cloud size and cloudy fraction) in an 11×11 pixel box centered on each cloudy pixel. An automated selection algorithm based on these parameters was developed to select cloudy pixels corresponding to the continental fair-weather cumulus. The selection algorithm was tested by a visual comparison to mixed cloud scenes.

The selection of cumulus based on geometry reduces the occurrence of aerosol that is misclassified as clouds [19]. Cloudy pixels were eliminated with optical thickness below 3 or effective radius below 4 μm, or if they contained ice or mixed phases. Cirrus contamination was eliminated by the use of the operational cloud-top pressure product based on CO_2 slicing. The surviving pixels were sorted into the following environmental bins based on satellite retrievals:

Total column precipitable water	From 3 to 4 cm at 1-km resolution.
Aerosol optical depth	From 0.2 to 0.4 at 10-km resolution.
Brightness temperature	From 298 to 270 K in 2° increments based on the 1-km resolution 11-μm emission. This is a proxy for the cloud-top altitude corresponding to a range of roughly 0.5 to 5 km above the surface.
Solar zenith angle	From 20° to 30° with the sun in the west, corresponding to early afternoon.

The data were then subdivided into observations within 45° of backscatter (illuminated pixels) and more than 45° from the backscatter (shadowed pixels), creating roughly equal sample sizes for comparison with the full data set. The 1-km-resolution effective radius data were averaged within each 2° temperature bin.

IV. Analysis

Aircraft observations in Amazonia demonstrate that cloud drop effective radius is a very stable variable as a function of altitude throughout an ensemble of neighboring cumulus clouds in various stages of development [20]. An ensemble of cloud-top properties thus reflects the development cycle of cumulus clouds. Since the microphysics of cumulus clouds is strongly correlated with vertical development, the data should be plotted in a manner that exhibits this dependence [1], [21]. Such a plot appears in Fig. 4(a), with cloud-top brightness temperature on the vertical and average effective radius on the horizontal. The solid line shows the full data set, with the illuminated subset plotted as a dashed line and the shadowed subset as a dotted line. The number of pixels averaged into each point is shown to the right [Fig. 4(a')]. As expected for an ensemble of moderately convective systems (fair-weather cumulus), the number of cloud-top pixels peaks at low altitude.

It is commonly assumed that the 3-D nature of clouds is manifested by their edges, and so the removal of edge pixels at 1-km resolution should substantially decrease the 3-D biases. This is implemented in newer versions of the cloud product (Collection 5) [22]. Fig. 4(b) and (b') is the same as Fig. 4(a) and (a') with all edge pixels removed. The pattern is essentially the same in both plots, although all effective radius values

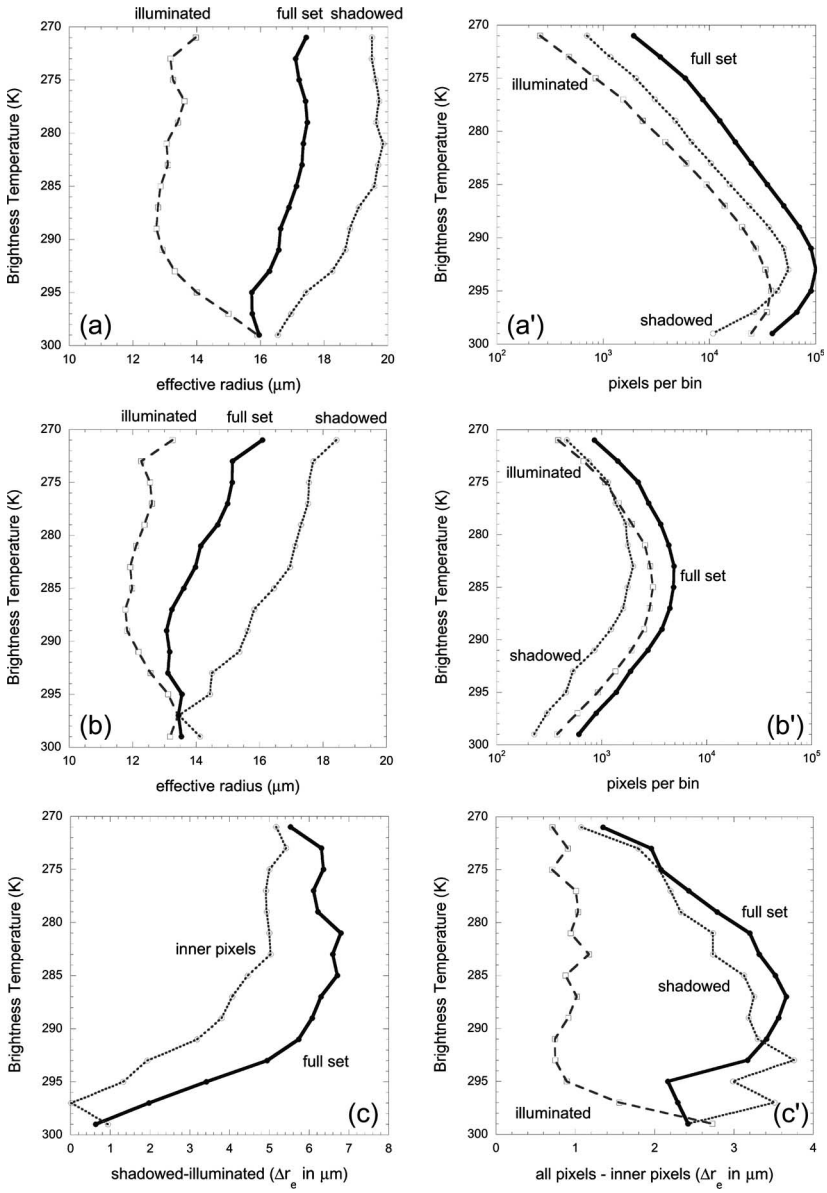

Fig. 4. Scattering angle and effective radius retrievals. The full data set of cloudy pixels is divided into backscatter (illuminated) and sidescatter (shadowed) subsets. The backscatter subset includes pixels within 45° of direct backscatter, and the sidescatter subset includes all other pixels. (a) Plots of effective radius as a function of (left) cloud-top brightness temperature with (right) the number of pixels averaged into each bin. (b) Same as (a) but with edge pixels removed (inner pixel subset). (c) Comparisons between the full data set and the subset with edge pixels removed. (Left) Difference between the average values of the shadowed and the illuminated pixel subsets. The solid and dotted lines indicate the full and inner data sets. (Right) Arithmetic difference between the average values of the two sets. The line styles are the same as in (a) and (b).

are smaller in Fig. 4(b) than in Fig. 4(a). The reasons for the common pattern and the effect when edge pixels are removed will be discussed in turn.

The general pattern of the effective radius plots of Fig. 4(a) and (b) fits the theory of diagram 2. As expected, the retrieved r_{e} is smaller or larger depending on whether it is illuminated or in shadow, and the difference between these two subsets may be taken as a measure of the 3-D nature of the cumulus clouds. Plots of this 3-D difference appear in Fig. 4(c) for the data sets of Fig. 4(a) and (b). Proceeding upward from the shallowest clouds at the bottom of the plot, the shadowed and illuminated values of r_{e} diverge from a common point before saturating at a roughly fixed separation from each other at $\sim$285 K. This saturation is likely due to the clouds on average maintaining a constant vertical/horizontal aspect ratio as they grow, so that the directional reflectance function is independent of the cloud size.

If this separation between scattering data represents 3-D biases of the retrieval, the lower portion indicates a progressive decline of the 3-D nature of the cumulus clouds as they become shallower. This decline could occur for two reasons. First, clouds of low optical thickness cannot sustain the contrast between the shadowed and illuminated portions. This is equivalent to a moving point P to the far left of the lookup table of Fig. 2. The dotted and dashed lines would simply follow the contours of the constant effective radius, and there would be no difference between the shadowed and illuminated values of r_{e}. A second possibility is that the 3-D effects are

expected to be greatest at cloud edges, and shallow clouds may have thin edges compared to the top surfaces. Reduction of the shadowing/illumination contrast does not necessarily mean that the retrieved data are closer to physical reality, for surface contamination becomes an important issue for shallow clouds [15].

The convergence of retrieved r_e with decreasing altitude for the shallow clouds of Fig. 4(a) and (b) represents variation in retrieval bias; but taken out of context, the different slopes of the right and left branches may be mistaken for physical reality. Between the unstable retrieval and surface contamination issues, such shallow clouds should be treated with caution and may not be usable. On the other hand, if the saturation of the 3-D biases for well-developed clouds is a universal tendency, these higher cloud tops may be used despite the bias if a consistent scattering geometry is maintained. The average retrieved effective radius would have an unknown but constant offset from the physically correct value.

The removal of cloud edge pixels is meant to reduce the 3-D bias on the pixel scale and surface contamination from the partially filled pixels [10]. Their presence can be detected by the differing influence on retrieved r_e: the 3-D scattering effects cause overestimation or underestimation depending on the scattering angle, while for all, but the thinnest cloud-surface contamination always causes overestimation for the 2.1-μm retrieval over vegetation [15]. Fig. 4(c) shows that the difference between shadowing and illumination retrievals in the saturated region decreases from 7 to 5 μm when the edge pixels are removed. This reduction in bias may not be entirely due to the 3-D cloud scattering effects, for surface contamination is reduced as well. This can be seen by the fact that averages for both shadowed and illuminated subsets decrease when the edge pixels are removed.

Finally, Fig. 4(c') shows the difference between the averages of the full set and the interior subset of pixels for the various scattering geometries. The removal of the edges has a much larger effect for the shadowing geometry, as might be predicted from the nonlinear response discussed for Fig. 2. It is also possible that although cloud edges should always be darker than the interior points in the shadowing geometry, they may not always be brighter in the illuminated geometry. As before, the different responses of the illuminated and shadowed data should not be interpreted purely as a cloud scattering effect, for the contribution from surface effects is a purely positive bias that will augment the shadowing bias while partially canceling out the negative bias from illumination. Even with a modeling study [10], it is not easy to say, when the edge pixels are removed, what proportion of the changes in retrieval values is due to the surface contamination versus the 3-D scattering effects. What we can say is that most of the differences between the shadowed and illuminated retrievals remain when the edge pixels are removed, and so are likely attributed to the subpixel structure.

The saturation of the 3-D biases for well-developed clouds [Fig. 4(a) and (b)] opens the possibility of a new analysis tool: data sets with the same amount of separation between the shadowed and illuminated pixels might be assumed to have an equivalent geometry, so they may be compared because they are biased equally. It should be possible to develop the theoretical correction factors based on scattering geometry for cloud ensembles that exhibit this saturation. A weighted average based on these correction factors would allow nearly all the data to be used instead of being limited to ensembles of fixed scattering geometry.

Cloud variability prevents a similar solution for individual scenes because such cloud ensembles are not large enough for a statistical correction to work. Yet, an understanding of the 3-D effects provides some guidance for experiment geometries that may minimize the bias. The goal is to find a viewing arrangement by which the visible and NIR reflectances from an actual cloud are the same as the theoretical reflectances from a plane-parallel cloud with the same effective radius and optical thickness. For the plane-parallel clouds, the brightest illumination occurs when the sun is directly overhead. The reflectance of 3-D clouds will be reduced in this geometry due to light leakage through the sides. But for these clouds, a bright spot will appear in the backscatter as the sun moves away from directly overhead. If the cloud is sufficiently thick, it is possible that this bright spot could meet or exceed the reflectance of the equivalent plane-parallel cloud despite light leakage. This means that so long as the solar zenith angle is sufficiently large and the clouds are sufficiently thick, a correctly positioned satellite could measure reflectances that match the plane-parallel equivalent. This position would be at or near backscatter, but the exact placement depends critically on the cloud geometry, optical thickness, and even the surface properties. Without knowledge of these quantities, the biases cannot be removed but may be standardized by requiring consistent experimental conditions across various scenes in a study.

V. Conclusion

Retrieval biases due to 3-D geometry of clouds were investigated with reference to shadowing and illumination. When the satellite is in the backscatter position relative to the sun, it will only view the illuminated portions of the cloud, and the effective radius retrieval will be smaller than the physically correct value. As the satellite moves away from the backscatter position, the shadowed portions will dominate the field of view, and the retrieved effective radius will increase. For the study of the cumulus clouds in Amazonia, a dividing line between the shadowed and illuminated clouds was set at 45° from the backscatter to create roughly equally sized subsets. The difference between the averages of the shadowed and the illuminated subsets for developed clouds was roughly 7 μm.

The elimination of the edge pixels at 1-km resolution only partially reduced the 3-D effects to a difference of 5 μm, indicating that subpixel structure plays a dominant role in the contrast between the shadowed and illuminated pixel retrievals. There is an additional effect: all effective radius averages decrease regardless of scattering angle, suggesting that surface contamination influences edge-pixel retrievals nearly as strongly as the 3-D scattering effects.

For the shallow clouds, the retrieval averages between the shadowed and illuminated pixels converged, representing a loss of 3-D characteristics. This change in effective radius bias with vertical development could be mistaken for a physical trend.

Such false trends might contaminate single-scene studies as well as the type of ensemble study presented in this paper. For the well-developed clouds, the difference between the shadowed and illuminated data tends to saturate at a roughly constant value regardless of cloud-top height.

It is recommended that the scattering geometry be explicitly controlled in future studies. In general, comparisons should only be made between data ensembles that have similar cloud morphology and scattering geometry. Caution is warranted, therefore, when applying MODIS level 3 products to cumulus studies. If the saturation for well-developed clouds observed in this data set holds for other data sets, the cloud morphology may prove to be of a less concern than scattering geometry. For such cases, cumulus clouds have enough scale similarities that theoretical correction factors might be devised based on the scattering angle alone. Such correction factors would only apply to large-scale statistics, not to individual scenes.

The current cloud retrieval algorithms are best suited for stratocumulus studies, making collocated retrievals of environmental variables (such as aerosol and precipitable water, which require cloud-free pixels) problematic. This severely limits satellite studies of interactions between the clouds and the environment. Further development along the lines indicated in this paper is needed to adapt current data sets to the study of scattered cumulus.

REFERENCES

[1] D. Rosenfeld and I. Lensky, "Satellite-based insights into precipitation formation processes in continental and maritime convective clouds," *Bull. Amer. Meteorol. Soc.*, vol. 79, no. 11, pp. 2457–2476, Nov. 1998.

[2] G. Stephens, "Cloud feedbacks in the climate system: A critical review," *J. Climate*, vol. 18, no. 2, pp. 237–273, Jan. 2005.

[3] H. Iwabuchi and T. Hayasaka, "Effects of cloud horizontal inhomogeneity on the optical thickness retrieved from moderate-resolution satellite data," *J. Atmos. Sci.*, vol. 59, no. 14, pp. 2227–2242, Jul. 2002.

[4] T. Nakajima and M. King, "Determination of the optical thickness and effective particle radius of clouds from reflected solar radiation measurements. Part 1: Theory," *J. Atmos. Sci.*, vol. 47, no. 15, pp. 1878–1893, Aug. 1990.

[5] N. Loeb and J. Coakley, "Inference of marine stratus cloud optical depths from satellite measurements: Does 1D theory apply?" *J. Climate*, vol. 11, no. 2, pp. 215–233, Feb. 1998.

[6] J. Coakley and C. Walsh, "Limits to the aerosol indirect radiative effect derived from observations of ship tracks," *J. Atmos. Sci.*, vol. 59, no. 3, pp. 668–680, Feb. 2002.

[7] T. Varnai and A. Marshak, "Observations of three-dimensional radiative effects that influence MODIS cloud optical thickness retrievals," *J. Atmos. Sci.*, vol. 59, no. 9, pp. 1607–1618, May 2002.

[8] ——, "Observations of three-dimensional radiative effects that influence satellite retrievals of cloud properties," *Q. J. Hung. Meteorol. Serv.*, vol. 106, no. 1, pp. 265–278, 2002.

[9] A. Marshak, S. Platnick, T. Varnai, G. Wen, and R. F. Cahalan, "Impact of 3D radiative effects on satellite retrievals of cloud droplet sizes," *J. Geophys. Res.*, vol. 111, D09207, 2006. DOI: 10.1029/2005JD006686.

[10] S. Kato, L. M. Hinkelman, and A. Cheng, "Estimate of satellite-derived cloud optical thickness and effective radius errors and their effect on computed domain-averaged irradiances," *J. Geophys. Res.*, vol. 111, D17201, 2006. DOI: 10.1029/2005JD006668.

[11] C. Cornet, H. Isaka, B. Guillemet, and F. Szczap, "Neural network retrieval of cloud parameters of inhomogenous clouds from multispectral and multiscale radiance data: Feasibility study," *J. Geophys. Res.*, vol. 109, D12203, 2004. DOI:10.1029/2003JD004186.

[12] H. Iwabuchi and T. Hayasaka, "A multi-spectral non-local method for retrieval of boundary layer cloud properties from optical remote sensing data," *Remote Sens. Environ.*, vol. 88, no. 3, pp. 294–308, Dec. 2003.

[13] Y. Kaufman and R. Fraser, "The effect of smoke particles on clouds and climate forcing," *Science*, vol. 277, no. 5332, pp. 1636–1639, Sep. 1997.

[14] G. Feingold, L. A. Remer, J. Ramaprasad, and Y. Kaufman, "Analysis of smoke impact on clouds in Brazilian biomass burning regions: An extension of Twomey's approach," *J. Geophys. Res.*, vol. 106, no. D19, pp. 22 907–22 922, Oct. 2002.

[15] D. Rosenfeld, E. Cattani, S. Melani, and V. Levizzani, "Considerations on daylight operation of 1.6 versus 3.7 μm channel on NOAA and METOP satellites," *Bull. Amer. Meteorol. Soc.*, vol. 85, no. 6, pp. 873–881, Jun. 2004.

[16] M. King, W. Menzel, Y. Kaufman, D. Tanre, B.-C. Gao, S. Platnick, S. Ackerman, L. Remer, R. Pincus, and P. Hubanks, "Cloud and aerosol properties, precipitable water, and profiles of temperature and water vapor from MODIS," *IEEE Trans. Geosci. Remote Sens.*, vol. 41, no. 2, pp. 442–458, Feb. 2003.

[17] S. Platnick, M. King, S. Ackerman, W. Menzel, B. Baum, J. Ridi, and R. Frey, "The MODIS cloud products: Algorithms and examples from Terra," *IEEE Trans. Geosci. Remote. Sens.*, vol. 41, no. 2, pp. 459–473, Feb. 2003.

[18] L. Remer, Y. Kaufman, D. Tanre, S. Mattoo, D. Chu, J. Martins, R.-R. Li, C. Ichoku, R. Levy, R. Kleidman, T. Eck, E. Vermote, and B. Holben, "The MODIS aerosol algorithm, products, and validation," *J. Atmos. Sci.*, vol. 62, no. 4, pp. 947–973, Apr. 2005.

[19] J. Brennan, Y. Kaufman, I. Koren, and R. R. Li, "Aerosol-cloud interaction—Misclassification of MODIS clouds in heavy aerosol," *IEEE Trans. Geosci. Remote Sens.*, vol. 43, no. 4, pp. 911–915, Apr. 2005.

[20] E. Freud, D. Rosenfeld, M. Andreae, A. Costa, and P. Artaxo, "Robust relations between CCN and the vertical evolution of cloud drop size distribution in deep convective clouds," *Atmos. Chem. Phys. Discuss.*, vol. 5, no. 5, pp. 10 155–10 195, 2005.

[21] I. Koren, Y. J. Kaufman, D. Rosenfeld, L. A. Remer, and Y. Rudich, "Aerosol invigoration and restructuring of Atlantic convective clouds," *J. Geophys. Res. Lett.*, vol. 32, LI4828, 2005. DOI: 10.1029/2005GL023187.

[22] M. King, S. Platnick, P. Hubanks, G. Arnold, E. Moody, G. Wind, and B. Wind, *Collection 005 Change Summary for the MODIS Cloud Optical Property (o6-OD) Algorithm*. [Online]. Available: http://modis-atmos.gsfc.nasa.gov/C005_Changes/C005_CloudOpticalProperties_ver311.pdf

Brian Vant-Hull received the B.S. degree in physics from Pomona College, Claremont, CA, and the M.A. degree in physics from the Johns Hopkins University, Baltimore, MD. He is currently working toward the Ph.D. degree in meteorology at the University of Maryland, College Park.

He has been recently relocated to the NOAA-CREST Center at the City University of New York to develop techniques for thunderstorm nowcasting.

Alexander Marshak received the M.S. degree in applied mathematics from Tartu University, Tartu, Estonia, in 1978, and the Ph.D. degree in numerical analysis from the Soviet Academy of Sciences, Moscow, Russia, in 1983.

In 1978, he joined the Institute of Astrophysics and Atmospheric Physics, Estonia and worked there for 11 years. In 1989, he received an Alexander von Humboldt fellowship and worked for two years with Gottingen University, Germany. He joined the Goddard Space Flight Center (GSFC), Greenbelt, MD, in 1991, working first with the SSAI then UMBC/JCET, and finally with the NASA/GSFC, where he has been employed since 2003. He has published over 90 refereed papers, books, and chapters in edited volumes.

Lorraine A. Remer received the B.S. and Ph.D. degrees in atmospheric science from the University of California, Davis, and the M.S. degree in oceanography from the University of California, San Diego, Scripps Institution of Oceanography, La Jolla.

She was with the NASA/Goddard Space Flight Center in 1991, employed by Science Systems and Applications Inc. until 1998 when she became a Civil Servant. Currently, she is a Physical Scientist with the Climate and Radiation Branch of Goddard's Laboratory for Atmospheres, Greenbelt, MD. She is a member of the EOS-MODIS science team and was a member of the Global Aerosol Climatology Project science team. Her current research interests are the climatic effects and remote sensing of atmospheric aerosol. She has been involved in several field campaigns including the smoke/sulfate, cloud and radiation experiments, the tropospheric aerosol radiative forcing observational experiment, the Israeli Desert Transition Zone experiment, the Puerto Rico Dust Experiment, and the Chesapeake Lighthouse Airborne Measurements for Satellites, as well as INTEX-B.

Zhanqing Li received the B.Sc. and M.Sc. degrees from the Nanjing Institute of Meteorology, Nanjing, China, in 1983 and 1985, respectively, and the Ph.D. degree from McGill University, Montreal, QC, Canada, in 1991.

After one year of postdoctoral research at the Meteorological Service of Canada, he joined the Canada Center for Remote Sensing as a Research Scientist. In 2001, he became a Professor at the Department of Atmospheric and Oceanic Science, University of Maryland, College Park, where he is also affiliated with the Earth Systems Sciences Interdisciplinary Center. He has been engaged in numerous meteorological and interdisciplinary studies concerning cloud, radiation budget, aerosol, UV radiation, terrestrial environment, forest fire, and carbon budget cycle. He has authored more than 110 peer-reviewed articles.

Dr. Li has received numerous merit awards.